

# Tissue distribution of polaprezinc in rats determined by the double tracer method

Shigeru Furuta \*, Michio Suzuki, Seiji Toyama, Masahiro Miwa, Hiroshi Sano

Central Research Laboratories Zeria Pharmaceutical Co., Ltd., 2512-1 Oshikiri, Konan-machi, Osato-gun,  
Saitama 360-0111, Japan

Received 8 May 1998; received in revised form 2 July 1998; accepted 8 July 1998

## Abstract

The tissue distribution of polaprezinc (an insoluble zinc complex of L-carnosine) in rats was studied by the double tracer method using [U- $^{14}\text{C}$ -histidine]-,  $^{65}\text{Zn}$ -polaprezinc. The  $^{65}\text{Zn}$ -radioactivity was measured with an auto-gamma counter, and the  $^{14}\text{C}$  containing  $^{65}\text{Zn}$  was converted to an absolute count according to the calibration curve for quenching with a liquid scintillation counter with the spill-over method. After the administration of  $^{14}\text{C}$ -,  $^{65}\text{Zn}$ -polaprezinc to rats, the excretion ratio and time courses in the tissues of the  $^{14}\text{C}$ - and  $^{65}\text{Zn}$ -radioactivity were different each other. We found that polaprezinc was metabolized as endogenous amino acid or zinc after dissociation in the body. The zinc concentration in plasma reached its maximum at 1 h and decreased slowly, returning to the endogenous level at 11 h after the administration of non-labeled polaprezinc. The concentrations of zinc in liver, kidney, testis, prostate, and cerebrum remained rather constant. The replacement ratios of  $^{65}\text{Zn}$  to zinc in the tissues at its maximum percentage were 40% in plasma, 16–20% in liver, kidney, blood, and prostate. The low replacement ratios in testis and cerebrum (2–3%) suggested that zinc uptakes in testis and brain were regulated by the blood-testis-barrier and blood-brain-barrier, respectively. © 1999 Elsevier Science B.V. All rights reserved.

*Keywords:* Polaprezinc; L-Carnosine; Zinc; Tissue distribution; Double tracer method

## 1. Introduction

Polaprezinc is a zinc complex of carnosine ( $\beta$ -alanyl-L-histidine) [1] that exhibits marked anti-ulcer activity by acting directly on the gastric mucosa [2–4]. Polaprezinc was found to be retained as the complex form in the stomach longer

and to adhere to the ulcerous sites more than did a mixture of zinc and L-carnosine for pharmacological action [5]. Polaprezinc is then dissociated to zinc and L-carnosine in the gastrointestinal tract as a function of time, and these components are further metabolized along their respective pathways in the body [6–8]. The tissue distribution of a drug is closely correlated with toxicological responses to the drug; a radiolabeled compound is useful to clarify tissue distribution, which is also important in the establishment of a

\* Corresponding author.

drug's disposition. In this study, we investigated the disposition of polaprezinc after oral administration to intact rats and discussed the toxicology and physiological roll of L-carnosine and zinc in tissues. Therefore, we synthesized [U- $^{14}\text{C}$ -histidine]-,  $^{65}\text{Zn}$ -polaprezinc, which labels L-carnosine as  $^{14}\text{C}$  and zinc as  $^{65}\text{Zn}$ , respectively, and determined the tissue levels of radioactivity using the double tracer method.

Furthermore, the distribution of zinc after the administration of non-labeled polaprezinc was compared to that of  $^{65}\text{Zn}$  to clarify the turnover of zinc, because zinc is distributed to all tissues, and the tissue concentrations of zinc are maintained by specific homeostatic mechanisms [9,10].

## 2. Materials and methods

### 2.1. Chemicals

Unlabeled polaprezinc and L-carnosine were synthesized by Hamari Chemicals (Tokyo, Japan). [U- $^{14}\text{C}$ -Histidine]-polaprezinc ( $^{14}\text{C}$ -polaprezinc) and  $^{65}\text{Zn}$ -polaprezinc were synthesized by Nemoto and Co. (Tokyo) and Amersham International (Buckinghamshire, UK), as shown in Fig. 1.  $^{65}\text{ZnCl}_2$  hydrochloride solution was purchased from Du Pont NEN Research Products (Boston, MA). The  $^{14}\text{C}$ -polaprezinc had the specific radioactivity level of  $26.8 \text{ MBq mmol}^{-1}$  and a radiochemical purity of 96.6%. The  $^{65}\text{Zn}$ -polaprezinc had specific radioactivity levels of  $36.4 \text{ MBq mmol}^{-1}$  and  $608.2 \text{ MBq mmol}^{-1}$ , and the  $^{65}\text{ZnCl}_2$  had a specific radioactivity level of  $47.1$

$\text{MBq mmol}^{-1}$ . The quenching standards of  $^{14}\text{C}$  were obtained from Packard Instrument (Maiden, CT).

### 2.2. Measurement of radioactivity

The measurement of the scintillation spectrum was performed with a liquid scintillation spectrophotometer (TRI CARB Type MINAXI, Packard Instrument) connected to a multi-channel analyzer for 4096 channels (SEIKO EG&G, Tokyo). The output pulses from the spectrometer to the multi-channel analyzer were picked up from the coincidence circuit. The  $^{14}\text{C}$ -radioactivity was measured by a liquid scintillation spectrophotometer (TRI CARB Type 4640, Packard Instrument), and the  $^{65}\text{Zn}$ -radioactivity was measured by an auto-gamma counter (Type 5780, Packard Instrument).

### 2.3. Liquid scintillation spectra of $^{14}\text{C}$ and $^{65}\text{Zn}$

The liquid scintillation spectra were measured with the  $^{14}\text{C}$ -quenched standard ( $124\,500 \text{ dpm per vial}$ ) for  $^{14}\text{C}$ , and with the  $^{65}\text{Zn}$ -quenched standard ( $200\,000 \text{ dpm per vial}$ ) made from  $^{65}\text{ZnCl}_2$  added to 10 ml of Aquasol-2 (Du Pont NEN Research Products).

### 2.4. Efficiency correlation curve for $^{14}\text{C}$ based on quenching

The quenching standard for  $^{65}\text{Zn}$  ( $65\,827 \text{ dpm per vial}$ ) was prepared by adding 0.1 ml of a 0.1 N

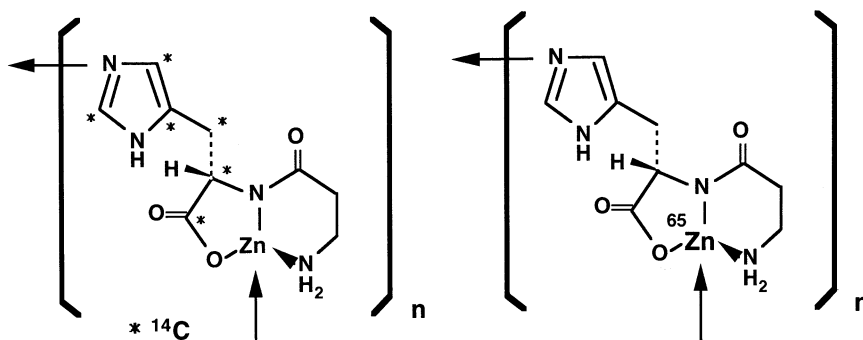


Fig. 1. Chemical structures of  $^{14}\text{C}$ -polaprezinc (left) and  $^{65}\text{Zn}$ -polaprezinc (right).

HCl solution of  $^{65}\text{Zn}$ -polaprezinc to biological samples (blood 0.1 or 0.2 ml, liver and lung both 200 mg). These were dissolved in 2 ml of soluene-350 (Packard), and to the samples of blood and liver was also added 0.4 ml of the saturated benzoyl peroxide in toluene, and 10 ml of Hionic flow (Packard). Each sample was evaluated by the analytical program of the  $^3\text{H}$ - and  $^{14}\text{C}$ -double labeling program with an automatic efficiency control (AEC) system [11], and the efficiency correlation curves for quenching were thus determined. The absolute radioactivity of  $^{14}\text{C}$  was obtained by the following equation:

$$C = (n\text{B} \cdot \text{EZA} - n\text{A} \cdot \text{EZB}) / (\text{ECB} \cdot \text{EZA})$$

where  $C$  is the absolute radioactivity of  $^{14}\text{C}$ ,  $n\text{A}$  and  $n\text{B}$  are total counts in regions A and B, and ECB, EZA, and EZB are the efficiency values of  $^{14}\text{C}$  in region B,  $^{65}\text{Zn}$  in region A, and  $^{65}\text{Zn}$  in region B, respectively. The regions of measurement energy were automatically set at 0–12 keV for region A and at 12–156 keV for region B.

We examined the effect of the  $^{65}\text{Zn}$  on the measurement of  $^{14}\text{C}$  in the biological samples (blood 0.1 ml, liver and stomach both 200 mg) treated as described above with the addition of 0.1 ml of the standard solution of  $^{14}\text{C}$  (166 dpm) and a 0.1 N HCl solution of  $^{65}\text{Zn}$ -polaprezinc (733 dpm). The  $^{14}\text{C}$ -radioactivity of these samples was measured by the scintillation counter using the spill-over method with the efficiency correlation curve of  $^{14}\text{C}$  based on quenching. The accuracy was calculated from the difference between the found and spiked levels of  $^{14}\text{C}$ -radioactivity divided by the spiked  $^{14}\text{C}$ -radioactivity.

## 2.5. Method of administration

Male SPF rats of the Sprague–Dawley strain (7–8 weeks of age, body weight:  $\approx 250$  g) were purchased from Charles River Japan (Atsugi, Japan). Solid laboratory food (Charles River CRF-1) was purchased from Oriental Yeast (Tokyo), and the zinc content was  $52 \mu\text{g g}^{-1}$  of the diet. The rats were fasted for 16 h prior to the dosing but were allowed free access to water, and foods were given at 8 h after the dosing. The  $^{14}\text{C}$ -polaprezinc and  $^{65}\text{Zn}$ -polaprezinc were mixed

together and suspended in a 0.5% sodium carboxymethyl cellulose solution with the use of an agate mortar, and administered orally at a dose of  $171.6 \mu\text{mol (50 mg) kg}^{-1}$  ( $^{14}\text{C}$ -,  $^{65}\text{Zn}$ -polaprezinc). The specific radioactivity was adjusted by the addition of non-radioactive polaprezinc; the radioactivity was  $\approx 862.1 \text{ kBq ml}^{-1}$  for  $^{14}\text{C}$ -polaprezinc and  $\approx 1.2 \text{ Mbq ml}^{-1}$  for  $^{65}\text{Zn}$ -polaprezinc.

Rats were exanguinated from the abdominal aorta under ether anesthesia with the use of a heparin-treated syringe. The cerebrum, liver, kidneys, stomach, testes, and prostate were excised and weighed. The tissue samples were cut and small pieces were obtained ( $\approx 200$  mg). Plasma samples were obtained from the blood samples after centrifugation ( $3000 \times g$ , 10 min). Each sample was dissolved in 2 ml of Soluene-350, and the radioactivity of  $^{65}\text{Zn}$  and  $^{14}\text{C}$  was measured as described above.

For the measurement of the zinc concentration in the tissues, non-labeled polaprezinc was administered orally at a dose of  $171.6 \mu\text{mol (50 mg) kg}^{-1}$ , and the tissue samples obtained as described above were ashed; the zinc concentration was measured at 213.8 nm by an atomic absorption spectrometer (Model 180-60, Hitachi, Tokyo) with a hollow cathode (Zn) lamp [12]. The area under the concentration-time curve until 24 h after administration ( $\text{AUC}_{0-24 \text{ h}}$ ) was calculated by the trapezoidal method. The replacement ratio in each tissue was calculated from the  $\text{AUC}_{0-24 \text{ h}}$  of  $^{65}\text{Zn}$  divided by the  $\text{AUC}_{0-24 \text{ h}}$  of zinc after the administration of polaprezinc.

## 3. Results

### 3.1. Quenching and counting efficiency of $^{14}\text{C}$ and $^{65}\text{Zn}$

We investigated the beta decay spectra of  $^{14}\text{C}$  and  $^{65}\text{Zn}$  in the liquid scintillation counter. The spectrum of  $^{14}\text{C}$ , the higher energy radionuclide, was low and flat over the 0–156 keV range. In contrast, the spectrum of  $^{65}\text{Zn}$ , the lower energy radionuclide, was sharp, peaking at 0–12 keV.

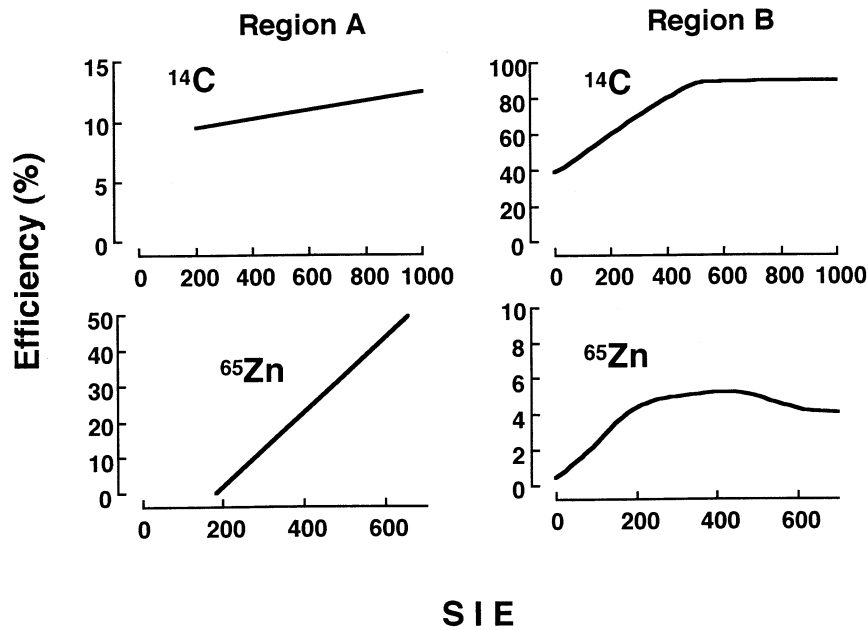


Fig. 2. Efficiency correlation curves of  $^{14}\text{C}$ -radioactivity and  $^{65}\text{Zn}$ -radioactivity for quenching in regions A and B.

The quenching and counting efficiency data of  $^{14}\text{C}$  and  $^{65}\text{Zn}$  in regions A and B are shown in Fig. 2. The efficiency of  $^{65}\text{Zn}$  was increased proportionally with spectral index of the external standard (SIE) in region A, and was  $< 5\%$  in region B. The efficiency of  $^{14}\text{C}$   $< 15\%$  in region A, but was  $> 70\%$  in region B when the SIE was  $> 260$ . The coefficients of variation of  $^{14}\text{C}$  and  $^{65}\text{Zn}$  in regions A and B obtained three times in the same samples by the efficiency correlation quenching curve were  $< 5\%$ .

### 3.2. Measurement precision of $^{14}\text{C}$ by the spill-over method in the presence of $^{65}\text{Zn}$

The measurement precision of  $^{14}\text{C}$ -radioactivity (166 dpm) in the stomach, liver, and blood samples in the presence of  $^{65}\text{Zn}$  (733 dpm) by the spill-over method is shown in Table 1. The values were similar to the  $^{14}\text{C}$ -radioactivity added; the accuracy was lower than 6.1%. The effects of the  $^{65}\text{Zn}$ -radioactivities on the analytical precision of  $^{14}\text{C}$  are shown in Table 2. The observed values of

$^{14}\text{C}$  were overestimated when the  $^{65}\text{Zn}$  radioactivities were 100 times  $> ^{14}\text{C}$  radioactivities. However, when the  $^{65}\text{Zn}$  radioactivities were 100 times  $< ^{14}\text{C}$  radioactivities,  $^{65}\text{Zn}$  did not interfere with the measurement of  $^{14}\text{C}$ , and the observed values were correct.

Table 1

The measurement of precision in the assay of  $^{14}\text{C}$ -radioactivity in tissue samples containing  $^{65}\text{Zn}$ <sup>a</sup>

Sample	SIE	$^{14}\text{C}$ radioactivity found (dpm)	Accuracy (%)
Blank	507	158	4.8
Blank	503	159	4.4
Stomach	424	156	6.0
Stomach	391	167	0.5
Liver	315	168	0.9
Liver	259	160	3.8
Blood	271	156	6.1
Blood	274	158	4.8
Mean		160	3.9
C.V (%)		2.9	

<sup>a</sup> Each sample contained  $^{14}\text{C}$  (166 dpm) and  $^{65}\text{Zn}$  (733 dpm).

Table 2  
The effect of  $^{65}\text{Zn}$ -radioactivity on the analysis of  $^{14}\text{C}$ -radioactivity in tissue samples<sup>a</sup>

$^{65}\text{Zn}$ -radioactivity added ( $\gamma$ dpm)	$^{14}\text{C}$ -radioactivity added ( $\beta$ dpm)	$^{14}\text{C}$ -radioactivity found ( $\beta$ dpm)	Accuracy (%)	Analysis time (min)
397		81 (4.2) <sup>b</sup>	3.3	10
733	81	82 (8.8)	6.2	10
1450		79 (5.8)	5.8	10
397		156 (5.8)	5.8	10
733	166	160 (2.9)	3.9	10
1450		149 (10.3)	10.3	10
1367		318 (4.8)	4.9	2
8440	329	321 (10.7)	7.7	2
33 927		322 (27.5)	18.5	2
1376		672 (3.3)	4.6	2
8440	702	680 (4.7)	4.5	2
33927		727 (12.9)	11.7	2
1376		1376 (2.5)	3.0	2
8440	1335	1407 (5.0)	6.4	2
33927		1393 (6.5)	11.13	2

<sup>a</sup> The tissue samples were prepared from blood, liver, and lung.

<sup>b</sup> Data are the mean (coefficient of variation, %), ( $n = 8$ ).

### 3.3. Distribution of $^{14}\text{C}$ -, $^{65}\text{Zn}$ -polaprezinc

The tissue distribution of  $^{14}\text{C}$ -,  $^{65}\text{Zn}$ -polaprezinc in the rats is shown in Fig. 3. The radioactivity of  $^{14}\text{C}$  in each tissue reached the maximum concentration ( $C_{\max}$ ) at 4–8 h after administration. The radioactivity of  $^{65}\text{Zn}$  reached the  $C_{\max}$  at 4 h in the plasma and blood, and at 8 h in the liver and kidney. The radioactivity of  $^{65}\text{Zn}$  in the prostate, testis, and cerebrum showed an increase as a function of time. The concentration of  $^{65}\text{Zn}$  in each tissue was lower than that of  $^{14}\text{C}$ . The zinc concentration in the plasma reached the  $C_{\max}$  at 1 h and decreased slowly, returning to the endogenous level at 11 h after the administration of non-labeled polaprezinc. In other tissues, the zinc concentration changed only slightly after the oral administration.

## 4. Discussion

The double tracer method using  $^{14}\text{C}$ -,  $^{65}\text{Zn}$ -polaprezinc (which is labeled by  $^{14}\text{C}$  in the L-carnosine moiety and labeled by  $^{65}\text{Zn}$  of the zinc

moiety) was useful in the present study, because the results of zinc and L-carnosine could be obtained from the same experiment at once. However, during the measurement of the pulse wave height and counts of  $^{14}\text{C}$  and  $^{65}\text{Zn}$  with the liquid scintillation spectrometer, we found that the spectra of  $^{14}\text{C}$  and  $^{65}\text{Zn}$  were crossed and interfered with each other. The multi-equation method [13] and the spill-over method [14] are used for the measurement of the mixture of two radio-labeled nuclei with a liquid scintillation spectrometer. The spill-over method uses the difference between the  $^3\text{H}$  and  $^{14}\text{C}$  spectra shapes. Since the  $^{65}\text{Zn}$  spectrum is similar to the  $^3\text{H}$  spectrum, we suspected that the spill-over method would be useful for the separate analyses of  $^{14}\text{C}$ - and  $^{65}\text{Zn}$ -radioactivity by a liquid scintillation spectrometer. In the examination of tissue distribution, each tissue sample was found to have its own color of quenching, and we investigated the relationship between the quenching and efficiency by the measurement of the quenching standard of  $^{14}\text{C}$  and  $^{65}\text{Zn}$ . The SIE is in inverse proportion to quenching; it is the index produced by analyzing the spectral distribution of the external standard. The efficiency of the

$^{65}\text{Zn}$ -radioactivity measurement was proportional to SIE under region A (the low energy area), and was very low under region B (the high energy area). The efficiency of the  $^{14}\text{C}$ -radioactivity measurement was  $\approx 10\%$  under region A, but was more than 70% under region B at high SIE values ( $> 260$ ), which is 20–30 times higher than those of  $^{65}\text{Zn}$ . Based on these data, we speculated that the measurement of  $^{14}\text{C}$ -radioactivity at region B by the liquid scintillation spectrometer was slightly affected by the  $^{65}\text{Zn}$ -radioactivity. We obtained the absolute amount of  $^{14}\text{C}$ -radioactivity by the measurement of  $^{14}\text{C}$ -radioactivity on region B, corrected with the efficiency correlation curve for quenching, by the spill-over method.

In our examination of the effect of  $^{65}\text{Zn}$  on the measurement of  $^{14}\text{C}$  in the various quenched biological samples such as blood, liver, and stomach, there were no effects of quenching or of  $^{65}\text{Zn}$ ; the accuracy of the measurement of  $^{14}\text{C}$  was  $< 6.1\%$ . Among the samples in which the ratio of  $^{14}\text{C}:$

was changed, the accuracy of measurement was less than 10.3% in the samples in which the  $^{65}\text{Zn}$ -radioactivity was not more than 20 times the  $^{14}\text{C}$ -radioactivity. The samples which had more than 300 dpm of  $^{14}\text{C}$ -radioactivity were measured accurately with a measurement period of 2 min. Webb et al. [15] measured the  $^{65}\text{Zn}$ -radioactivity and Cousins et al. [16] measured both  $^{14}\text{C}$ - and  $^{65}\text{Zn}$ -radioactivity with a liquid scintillation spectrometer. Since the present maximum of efficiency of  $^{65}\text{Zn}$  in region A was only 42.7% (Fig. 2),  $^{65}\text{Zn}$  was more influenced by quenching than  $^{115\text{m}}\text{Cd}$  or  $^{203}\text{Hg}$  [16]. It is difficult to measure the  $^{65}\text{Zn}$ -radioactivity in high-quenching samples such as blood or liver, because the efficiency of  $^{65}\text{Zn}$ -radioactivity is decreased greatly by the mixed  $^{14}\text{C}$ -radioactivity. Therefore, in the present study, we first measured the  $^{65}\text{Zn}$ -radioactivity with a gamma-counter, and then more accurately measured the  $^{14}\text{C}$ -radioactivity by the spill-over method with a liquid scintillation counter.

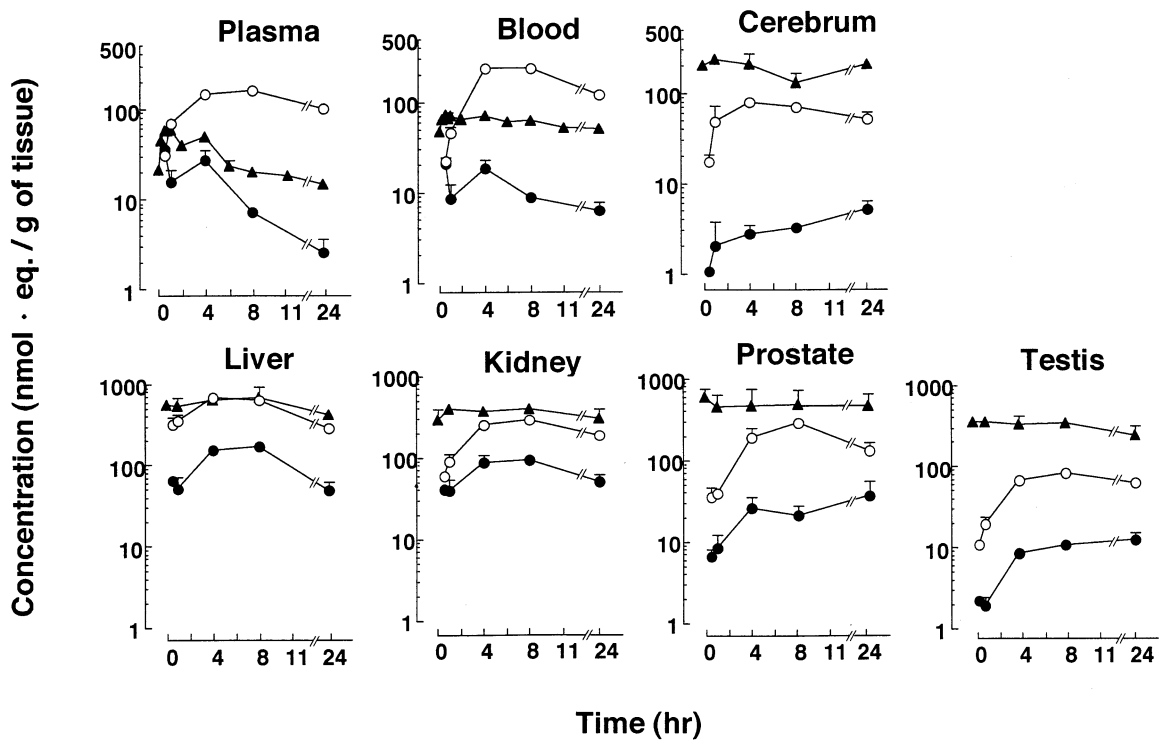


Fig. 3. Tissue distribution of polaprezinc after oral administration to rats ( $171.6 \mu\text{mol}$  ( $50 \text{mg}$ )  $\text{kg}^{-1}$ ). Each point represents the mean  $\pm$  SD: (○)  $^{14}\text{C}$ -radioactivity ( $n = 3$ ), (●)  $^{65}\text{Zn}$ -radioactivity ( $n = 3$ ), (▲) Zinc ( $n = 5$ ).

Table 3  
Pharmacokinetic parameters of polaprezinc after oral administration to rats (171.6  $\mu$  mol (50 mg)  $\text{kg}^{-1}$ )

Tissue	Nuclide	$T_{\max}$ (h)	$C_{\max}$ (nmol eq. $\text{ml}^{-1}$ or $\text{g}^{-1}$ )	$\text{AUC}_{0-24 \text{ h}}$ (ng eq. $\text{h ml}^{-1}$ )	Replacement ratio (%) <sup>a</sup>
Plasma	$^{14}\text{C}$	8	$161.15 \pm 17.51^{\text{b}}$	3.71.94	40.70
	$^{65}\text{Zn}$	4	$27.00 \pm 7.84$	231.62	
	Zinc	1	$59.35 \pm 5.66$	569.07	
Blood	$^{14}\text{C}$	8	$233.53 \pm 22.00$	4197.15	16.94
	$^{65}\text{Zn}$	4	$18.54 \pm 4.21$	227.74	
	Zinc	0.5	$71.29 \pm 4.28$	1344.46	
Cerebrum	$^{14}\text{C}$	4	$78.14 \pm 8.25$	1489.47	2.04
	$^{65}\text{Zn}$	24	$5.21 \pm 1.14$	87.62	
	Zinc	1	$232.94 \pm 33.40$	4292.51	
Liver	$^{14}\text{C}$	4	$673.17 \pm 92.16$	11670.7	20.10
	$^{65}\text{Zn}$	8	$168.47 \pm 17.78$	2727.54	
	Zinc	8	$671.99 \pm 243.60$	13568.70	
Kidney	$^{14}\text{C}$	8	$283.81 \pm 7.42$	5387.11	20.28
	$^{65}\text{Zn}$	8	$91.78 \pm 8.91$	1713.58	
	Zinc	8	$387.97 \pm 37.87$	8448.81	
Prostate	$^{14}\text{C}$	8	$290.50 \pm 49.59$	4711.06	16.11
	$^{65}\text{Zn}$	24	$36.88 \pm 18.47$	616.53	
	Zinc	24	$500.08 \pm 185.71$	3826.25	
Testis	$^{14}\text{C}$	8	$83.89 \pm 6.35$	1611.99	3.25
	$^{65}\text{Zn}$	24	$12.29 \pm 3.14$	239.55	
	Zinc	1	$350.58 \pm 12.93$	7376.82	

<sup>a</sup> Replacement ratios were calculated from  $\text{AUC}_{0-24 \text{ h}}$  of  $^{65}\text{Zn}$  divided by  $\text{AUC}_{0-24 \text{ h}}$  of zinc after administration.

<sup>b</sup> Data are the mean  $\pm$  SD ( $^{14}\text{C}$  and  $^{65}\text{Zn}$ :  $n = 3$ , Zinc:  $n = 5$ ).

After oral administration of  $^{14}\text{C}$ -,  $^{65}\text{Zn}$ -polaprezinc to rats, the distributions of  $^{14}\text{C}$ - and  $^{65}\text{Zn}$ -radioactivity in each tissue showed independence. We reported that polaprezinc administered was not dissociated immediately, and was present in its complex form in the stomach at 30 min after administration [5,8]. After that, most of dose of polaprezinc was dissociated to zinc and L-carnosine in the gastrointestinal tract as a function of time [8], we could detect the radioactivity of  $^{14}\text{C}$  and  $^{65}\text{Zn}$  as L-carnosine and zinc, respectively. Furthermore, L-carnosine was metabolized rapidly to L-histidine and  $\beta$ -alanine in rats [17], we could not detect L-carnosine in plasma after administration of polaprezinc [18]. The  $^{14}\text{C}$ -radioactivity remained in the tissues at 24 h after administration, it suggested that L-histidine as metabolites of L-carnosine was incorporated by endogenous high molecular weight substances

such as protein [17]. We reported the absorption of  $^{65}\text{ZnSO}_4$  in rats previously, the times of maximum concentration ( $T_{\max}$ ) of  $^{65}\text{Zn}$ -radioactivity in plasma were 1 h of  $^{65}\text{ZnSO}_4$  [8], and 4 h of polaprezinc after oral administration to rats, respectively. It suggested that the absorption of zinc after administration of polaprezinc was slowly than that of  $^{65}\text{ZnSO}_4$ , because it requires the dissociation time. The  $^{65}\text{Zn}$ -radioactivity showed a high distribution in the liver and kidney, and showed time-dependent increases in the prostate, testis, and cerebrum. The  $^{65}\text{Zn}$  replacement ratio was large (40%) in the plasma, 16–20% in the liver, kidney, blood, and prostate, and very low in the testis and cerebrum (Table 3). The zinc is an essential trace metal widely distributed to tissues [19]. The zinc of polaprezinc seems to be taken up into each tissue and metabolized with the turnover of endogenous zinc.

The zinc was absorbed by carrier-mediated process, as is copper, and it was regulated by the concentration of zinc in the intestine [20]. The testis and brain have a blood–testis-barrier [21] and blood–brain-barrier [22], respectively, which act to regulate the uptake of many substances into these tissues similar to the intestine. The LD<sub>50</sub> values of polaprezinc was 8441 mg kg<sup>-1</sup> in rats single oral administration study, it seemed safety though it include heavy metal, zinc [23]. Each tissue could prevented to the exposure of zinc in excess by the barriers system. These barriers regulate the zinc uptake homeostatically, and the replacement ratios of <sup>65</sup>Zn in the rat testis and cerebrum were thus found to be very low. In addition, time-dependent increases in the <sup>65</sup>Zn-radioactivity were observed in the prostate, testis and cerebrum. These results suggest that zinc has an important role in the production of sperm and is an essential metal in the regular functioning of the brain. In this study, we investigated the disposition of polaprezinc in intact rats. However, the physiological condition about the turnover or barrier system of zinc may be changed in the ulcer model rats. Therefore, it will be necessary to study using the ulcer model rats for discussion about the pharmacological response of polaprezinc.

## 5. Conclusion

After the administration of <sup>14</sup>C-, <sup>65</sup>Zn-polaprezinc to rats, the excretion ratio and time courses in the tissues of the <sup>14</sup>C- and <sup>65</sup>Zn-radioactivity were different each other. We found that polaprezinc was metabolized as endogenous amino acid or zinc after dissociation in the body. The concentrations of zinc in liver, kidney, testis, prostate, and cerebrum remained rather constant.

The replacement ratios of <sup>65</sup>Zn to zinc in the tissues at its maximum percentage were 40% in plasma, 16–20% in liver, kidney, blood, and prostate. The low replacement ratios in testis and cerebrum (2–3%) suggested that zinc uptakes in testis and brain were regulated by the blood-testis-barrier and blood–brain-barrier, respectively.

## References

- [1] T. Matsukura, T. Takahashi, Y. Nishimura, H. Sawada, K. Shibata, Characterization of crystalline L-carnosine Zn(II) complex (Z-103), a novel anti-gastric ulcer agent: tautomeric change of imidazole moiety upon complexation, *Chem. Pharm. Bull.* 38 (1990) 3140–3146.
- [2] T. Arakawa, H. Satou, A. Nakamura, et al., Effects of zinc L-carnosine on gastric mucosal and cell damage caused by ethanol in rats, *Dig. Dis. Sci.* 35 (1990) 559–566.
- [3] M. Ito, T. Tanaka, Y. Suzuki, Effect on *N*-(3-aminopropionyl)-L-histidine zinc (Z-103) on healing and hydrocortisone-induced relapse of acetic acid ulcers in rats with limited food-intake-time, *Jpn. J. Pharmacol.* 52 (1990) 513–521.
- [4] M. Seiki, S. Ueki, Y. Tanaka, et al., Studies on the anti-ulcer effects of a new compound, zinc L-carnosine (Z-103), *Folia Pharmacol. Jpn.* 95 (1990) 257–269.
- [5] S. Furuta, S. Toyama, M. Miwa, T. Itabashi, H. Sano, T. Yoneta, Residence time of polaprezinc (zinc L-carnosine) in the rat stomach and adhesiveness to ulcerous sites, *Jpn. J. Pharmacol.* 67 (1995) 271–278.
- [6] H. Sano, S. Furuta, S. Toyama, et al., Study on the metabolic fate of catena-(*S*)-[μ-(3-aminopropionyl) histidinato(2-)-*N*<sup>1</sup>,*N*<sup>2</sup>,*O*:*N*<sup>7</sup>]-zinc], 1st communication: absorption; distribution; metabolism; and excretion after single administration to rats, *Arzneim.Forsch. Drug Res.* 41 (1991) 965–975.
- [7] S. Furuta, S. Toyama, M. Miwa, H. Sano, Absorption property and disposition in gastrointestinal tract of zinc L-carnosine (Z-103), *J. Pharm. Dyn.* 15 (1992) S30.
- [8] S. Furuta, S. Toyama, M. Miwa, H. Sano, Disposition of polaprezinc (zinc L-carnosine complex) in rat gastro-intestinal tract and effect of cimetidine on its adhesion to gastric tissues, *J. Pharm. Pharmacol.* 47 (1995) 632–636.
- [9] N.T. Davies, Studies on the absorption of zinc by rat intestine, *Br. J. Nutr.* 43 (1980) 189–203.
- [10] M.J. Jackson, D.A. Jones, R.H. Edwards, Zinc absorption in the rat, *Br. J. Nutr.* 46 (1981) 15–27.
- [11] TRI-CARB 4000 Series Liquid Scintillation Systems Operation Manual. Packard Instrument Co., Inc. 1983.
- [12] S. Toyama, S. Furuta, M. Miwa, M. Suzuki, H. Sano, K. Matsuda, Study on the metabolic fate of catena-(*S*)-[μ-(3-aminopropionyl) histidinato(2-)-*N*<sup>1</sup>,*N*<sup>2</sup>,*O*:*N*<sup>7</sup>]-zinc], 2nd communication: absorption; distribution; metabolism; and excretion after repeated administration, *Arzneim. Forsch. Drug Res.* 41 (1991) 976–983.
- [13] G.T. Okita, J.J. Kabara, F. Richardson, G.B. Leroy, Assaying compounds containing <sup>3</sup>H and <sup>14</sup>C, *Nucleonics* 15 (1957) 111–114.
- [14] A. Viotti, R. Nucca, Double labeling: computation program for a desk-top calculator, *Anal. Bio.* 65 (1975) 556–560.
- [15] M. Webb, H. Creed, S. Atkinson, Influence of zinc on protein synthesis by polyribosomes from the dog prostate and dorsolateral lobes of the rat prostate, *Bio. Biophys. Acta* 324 (1973) 143–155.



- [16] R.J. Cousins, R.A. Wynbeen, K.S. Squibb, M.P. Richards, Double label counting of metal nuclides with  $^3\text{H}$  or  $^{14}\text{C}$  by liquid scintillation counting, *Anal. Bio.* 65 (1975) 412–417.
- [17] S. Furuta, S. Toyama, M. Miwa, H. Sano, Studies on the metabolic fate of L-carnosine in rats and humans, *Xenobiot. Metab. Dispos.* 8 (1993) 1057–1063.
- [18] S. Furuta, S. Toyama, M. Miwa, Y. Ikeda, H. Sano, K. Matsuda, Study on the metabolic fate of catena-(S)-[ $\mu$ -[N $^{\alpha}$ -(3-aminopropionyl) histidinato(2-)-N $^1$ ,N $^2$ ,O:N $^7$ ]-zinc], 4th communication: disposition of zinc and amino acids in rats; dogs; and monkeys, *Arzneim. Forsch. Drug Res.* 41 (1991) 992–995.
- [19] B.L. Vallee, K.H. Falchuk, The biochemical basis of zinc physiology, *Physiol. Rev.* 73 (1993) 79–118.
- [20] S. Furuta, S. Toyama, H. Sano, Absorption of polaprezinc (zinc L-carnosine complex) by an everted sac method, *Xenobiotica* 24 (1994) 1085–1094.
- [21] L.D. Russel, R.W. Peterson, Sertoricell junction : morphological and functional correlates, *Int. Rev. Cytol.* 94 (1985) 177–211.
- [22] G.W. Goldstein, Endothelial cell-astrocyte interactions: a cellular mod-brain bardel of the bloorier, *Ann. New York Acad. Sci.* 529 (1988) 1083–1090.
- [23] K. Matsuda, H. Shibata, T. Morikami, T. Kato, F. Aruga, Single dose toxicity study on catena-(S)-[ $\mu$ -[N $^{\alpha}$ -(3-aminopropionyl) histidinato(2-)-N $^1$ ,N $^2$ ,O:N $^7$ ]-zinc] in mice and rats, *Arzneim. Forsch. Drug Res.* 41 (1991) 1033–1035.